Publications of the Korean Astronomical Society
32: 293 ∼ 297, 2017 March

pISSN 1225-1534
eISSN 2287-6936
https://doi.org/10.5303/PKAS.2017.32.1.293

FAR INFRARED AND SUBMILLIMETRE SURVEYS: FROM IRAS TO AKARI, HERSCHEL AND PLANCK

Michael Rowan-Robinson[1] & Lingyu Wang[2]

[1]Blackett Laboratory, Imperial College London, London SE7 2AZ
[2]Institute for Computational Cosmology, Department of Physics, Durham University, South Road, Durham DH1 3LE, UK

E-mail: mrr@imperial.ac.uk

(Received July 21, 2015; Revised October 25, 2016; Accepted October 25, 2016)

ABSTRACT

We discuss a new IRAS Faint Source Catalog galaxy redshift catalogue (RIFSCz) which incorporates data from Galex, SDSS, 2MASS, WISE, AKARI and Planck. AKARI fluxes are consistent with photometry from other far infrared and submillimetre missions provided an aperture correction is applied. Results from the Hermes-SWIRE survey in Lockman are also discussed briefly, and the strong contrast between the galaxy populations selected at 60 and 500 μm is summarized.

Key words: infrared surveys - infrared galaxies - star formation - gravitational lensing

1. INTRODUCTION

With IRAS we were able to identify the main infrared galaxy populations: quiescent galaxies (infrared cirrus), starburst galaxies (prototype M82), extreme starbursts (prototype A220) and AGN dust tori (Rowan-Robinson & Crawford, 1989; Efstathiou & Rowan-Robinson, 1995). These templates were modelled with radiative transfer codes, which improved enormously with detailed mid-infrared spectroscopy from ISO (Rowan-Robinson & Crawford, 1989; Rowan-Robinson, 1992, 1995; Efstathiou & Rowan-Robinson, 1995; Efstathiou et al., 2000; Efstathiou & Rowan-Robinson, 2003; Silva et al., 1998; Popescu et al., 2000, 2011; Siebenmorgen & Krugel, 2007; Berta et al., 2013). One of the great benefits of radiative transfer modelling of galaxy infrared spectral energy distributions (SEDs) is that we can get accurate estimates of the star-formation rate and dust mass. If the optical-nir emission from stars is modelled with stellar synthesis model templates, we also get an estimate of the stellar mass (c.f. Rowan-Robinson et al., 2010, 2013).

Wang & Rowan-Robinson (2014) have compiled a new IRAS Faint Source Catalog galaxy redshift catalogue (RIFSCz) incorporating Galex, SDSS, 2MASS, WISE, AKARI and Planck data. The number of sources detected in different wavebands is summarized in Table 1. Section 3 gives a discussion of the AKARI sources.

2. MODELLING SEDs OF HERMES-SWIRE GALAXIES

Rowan-Robinson et al. (2014) have also embarked on a template-fitting study of all Hermes-SWIRE galaxies (>5000 galaxies), starting with a pilot study in the 7.5 sq deg Lockman area. There are 1331 5-σ 500 μm sources in the area surveyed by SWIRE and 967 of these have an association with a 24 μm source from the SWIRE Photometric Redshift Survey catalogue. The SEDs of these have been automatically fitted with a set of 6 infrared templates: standard cirrus, a cooler (15-20K) cirrus template, three starburst templates (M82, A220 and a young starburst template) and an AGN dust torus template. We have modelled the individual SEDs for several hundred of these, including those which gave a poor χ^2 in the automatic fit. Poor χ^2 are generally due either to the presence of cold dust (10-13K) or to the effects of gravitational lensing. Lensing candidates can be recognised through a set of colour-colour constraints. Figure 1 shows S500/S24 versus S3.6/S500 for Hermes-Lockman galaxies with 0.15<z<0.95, with lensing candidates shown in red and galaxies with a cold dust component shown in green. There is a clear sepa-

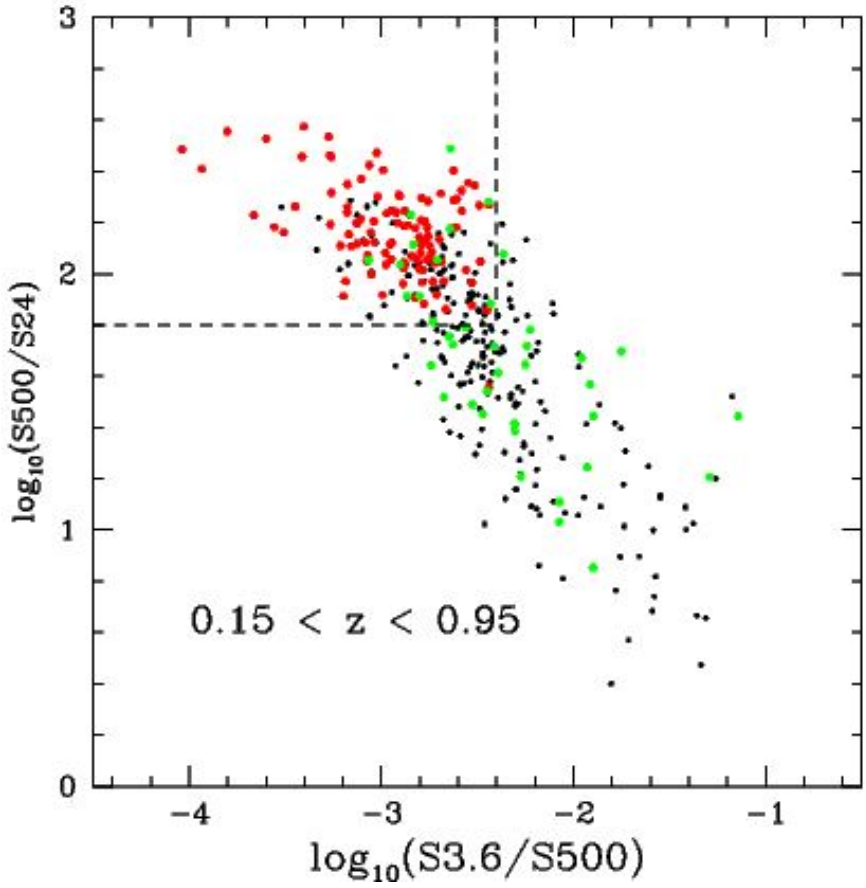

Figure 1. S24/S500 versus S3.6/S500 for Lockman-Hermes-SWIRE galaxies with 0.15<z<0.95. Red filled circles: lensing candidates, green filled circles: galaxies with cold cirrus component.

ration in this plot between galaxies with cold dust components and lensing candidates.

There is a great contrast between the galaxy populations selected at 500 μm (Herschel) and 60 μm (IRAS). At 500 μm 70% are ultraluminous, 26% are hyperluminous, 88% have z > 0.3 and 8% are lensing candidates. At 60μm 8% are ultraluminous, 0.7% are hyperluminous, and 4% have z > 0.3. Only 4 IRAS FSC galaxies (0.007%) are definitely known to be lensed. This difference is driven by the negative K-correction at submillimetre wavelengths (Franceschini et al., 1994; Blain et al., 1996).

3. AKARI SOURCES

The AKARI-FIS All-sky Bright Source Catalogue Yamamura et al. (2010) contains 427,071 sources at 65, 90, 140 and 160 μm. The most reliable sources are those associated with IRAS sources. 18153 AKARI 90μm sources (with reliability flag 3 and 3-σ detections) are associated with IRAS FSC galaxies, as are 857 65μm sources, 3601 140μm sources and 739 160μm sources (see Table 1). Earlier problems identified during AKARI catalogue check-out of discrepancies between AKARI and IRAS fluxes are now resolved by application of an aperture correction at 65 and 90μm. Figure 2 shows S100(IRAS)/S90(AKARI) versus the 2MASS J-band aperture correction delmag = $J_{ext} - J_{ps}$. The red line indicates the need for an aperture correction of 0.06×delmag to $log_{10}S90$.

The same correction is applied at 65μm but no correction seems to be needed at 140 and 160μm. Figure 3 shows SEDs of Planck galaxies requiring a cold dust component, with aperture-corrected AKARI fluxes shown in red. Figure 4 shows SEDs of RIFSCz nearby galaxies with poor χ^2 from their automatic template fits, this time with aperture-corrected AKARI fluxes shown in blue. AKARI fluxes now show good consistency with IRAS, WISE and Planck fluxes.

4. HISTORICAL FOOTNOTE ON 1.38 mm SOURCES

Finally Figure 5 provides a historical footnote. It shows a plot of S(1.38mm), labelled as S1380 in the Figure,

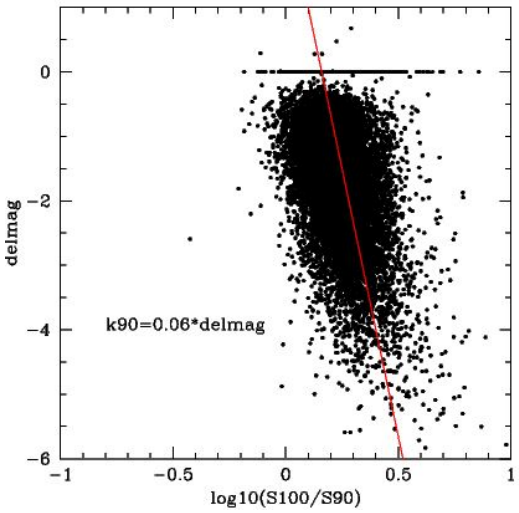

Figure 2. 2MASS J-band aperture correction, delmag, versus S90(AKARI)/ S100(IRAS), illustrating need for an aperture correction to the AKARI 90μm flux.

versus redshift for Planck sources (black filled circles), plus predicted fluxes from the RIFSCz template fits (red filled circles) and a few other fluxes from ground-based measurements (black triangles). Brighter sources have been labelled with the reference to their first detection: Rowan-Robinson et al. (1975), Ade et al. (1976), Hildebrand et al. (1977), Elias et al. (1978), Landau et al. (1983). Almost all sources brighter than 2 Jy were detected in the 1970s by the Queen Mary College and Caltech groups. No new non-radio IRAS sources at z>0.2 were detected in the Planck ERCSC.

Table 1
RIFSCz catalogue by band

$\lambda(\mu$m)	survey	no. of sources
3.4	WISE	48603
4.6	WISE	48603
12	WISE	48591
12	IRAS	4476
22	WISE	48588
25	IRAS	9608
60	IRAS	60303
65	AKARI	857
90	AKARI	18153
100	IRAS	30942
140	AKARI	3601
160	AKARI	739
350	PLANCK	2275
550	PLANCK	1152
850	PLANCK	616
1380	PLANCK	150

WISE gives 3.4-22 μm fluxes for 80% of IRAS 60μm galaxies. AKARI-FIS and PLANCK give 140-850μm fluxes for 1-6% of IRAS 60μm galaxies.

REFERENCES

Ade P.A.R., Rowan-Robinson M., Clegg P. E., 1976, A&A 53, 403

Berta S., et al, 2013, Panchromatic spectral energy distributions of Herschel sources, A&A, 551, 100

Blain A., 1996, Galaxy-galaxy gravitational lensing in the millimetre/submillimetre waveband, MNRAS, 283, 1340

Efstathiou A., Rowan-Robinson M., 1995, Dusty discs in active galactic nuclei, MNRAS, 273, 649

Efstathiou A. & Rowan-Robinson M., 2003, Cirrus models for local and high-z SCUBA galaxies, MNRAS, 343, 322

Efstathiou A., Rowan-Robinson M., Siebenmorgen R., 2000, Massive star formation in galaxies: radiative transfer models of the UV to millimetre emission of starburst galaxies, MNRAS, 313, 734

Elias J. H., et al., 1978, 1 millimeter continuum observations of extragalactic objects, ApJ, 220, 25

Franceschini A., Mazzei P., de Zotti G., Danese L., 1994, Luminosity evolution and dust effects in distant galaxies: Implications for the observability of the early evolutionary phases, ApJ, 427, 140

Hildebrand R. H., et al., 1977, Submillimeter photometry of extragalactic objects, ApJ, 216, 698

Landau R., et al., 1983, Extragalactic 1 millimeter sources - Simultaneous observations at centimeter, millimeter, and visual wavelengths, ApJ, 268, 68L

Popescu C. C., et al., 2000, Modelling the spectral energy distribution of galaxies. I. Radiation fields and grain heating in the edge-on spiral NGC 891, A&A, 362, 138

Popescu C. C., et al., 2011, Modelling the spectral energy distribution of galaxies. V. The dust and PAH emission SEDs of disk galaxies, A&A, 527, 109

Rowan-Robinson M., Clegg P., & E., Ade P. A. R., 1975, Millimetre emission from extragalactic objects. I - Observational techniques and data analysis, MNRAS, 172, 603

Rowan-Robinson M. & Crawford J., 1989, Models for infrared emission from IRAS galaxies, MNRAS, 238, 523

Rowan-Robinson M., 1992, Interstellar dust in galaxies, MNRAS, 258, 787

Rowan-Robinson M., 1995, A new model for the infrared emission of quasars, MNRAS, 272, 737

Rowan-Robinson M., et al., 2010, Cold dust and young starbursts: spectral energy distributions of Herschel SPIRE sources from the HerMES survey, MNRAS, 409, 2

Rowan-Robinson M., et al., 2013, Revised SWIRE photo-

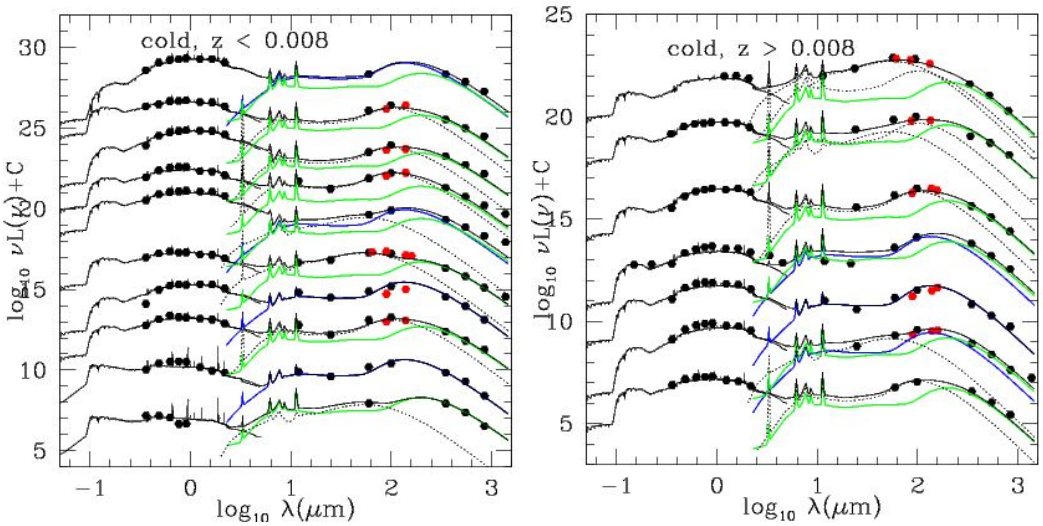

Figure 3. SEDs for Planck galaxies requiring a cold cirrus component, with aperture-corrected AKARI fluxes in red. Blue curves: cool cirrus, green curves: cold cirrus.

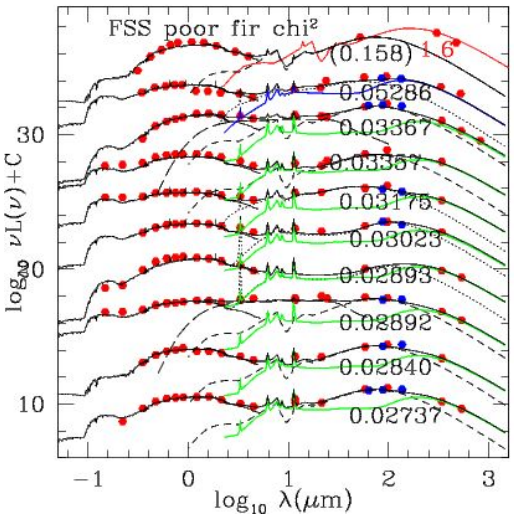

Figure 4. SEDs for RIFSCz galaxies with poor χ^2 from automatic fit, with aperture-corrected AKARI fluxes in blue. Blue curves: cool cirrus, green curves: cold cirrus, red curve: lensing candidate.

metric redshifts, MNRAS, 428, 1958

Rowan-Robinson M., et al., 2014, Detailed modelling of a large sample of Herschel sources in the Lockman Hole: identification of cold dust and of lensing candidates through their anomalous SEDs, MNRAS, 445, 3848

Siebenmorgen R. & Krugel E., 2007, Dust in starburst nuclei and ULIRGs. SED models for observers, AA, 461, 445

Silva, L., et al., 1998, Modeling the Effects of Dust on Galactic Spectral Energy Distributions from the Ultraviolet to the Millimeter Band, ApJ, 509, 103

Wang L., Rowan-Robinson M., 2014, The Revised IRAS-FSC Redshift Catalogue (RIFSCz), MNRAS 442, 2739

Yamamura I. et al., 2010, AKARI-FIS All-Sky Survey Point Source Catalogues (ISAS/JAXA)

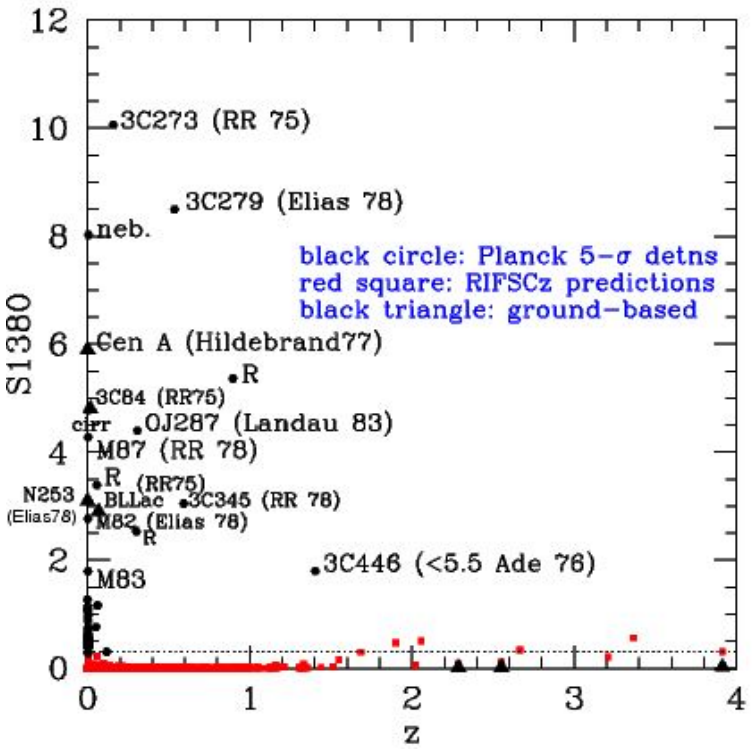

Figure 5. S(1.38mm) versus redshift for Planck ERCSC sources (filled black circles). Brighter sources are labelled with reference to their first detection. The red filled circles show predicted RIFSCz fluxes derived from the automatic SED fitting, black triangles denote modern ground-based measurements. The dotted line corresponds to the Planck detection limit.